MT-NMR method to diffusion in particles important in chromatography and in gel phase synthesis are in progress.

Acknowledgment. We thank the National Science Foundation for support through Grants DMR-8304251 (W.T.F.), DMR-8500704 (B.J.A.), and DMB-8603864 (to the Oklahoma State University Department of Chemistry for upgrade of the NMR spectrometer) and the donors of the Petroleum Research Fund, administered by the American Chemical Society, for support of the research of F.D.B. We thank M. P. Sudhakaran for help with Fortran programming.

Supplementary Material Available: Figures 4-12 showing simulated diffusion for the remainder of the experiments of Table I plotted as in Figures 2 and 3 (9 pages). Ordering information is given on any current masthead page.

Deuterium and Carbon-13 NMR of the Solid Polymorphism of Benzenehexoyl Hexa-*n*-hexanoate

E. Lifshitz,[†] D. Goldfarb,[†] S. Vega,[†] Z. Luz,*[†] and H. Zimmermann[‡]

Contribution from The Weizmann Institute of Science, Rehovot 76100, Israel, and Max-Planck-Institut für Medizinische Forschung, 6900 Heidelberg, West Germany.
Received December 15, 1986

Abstract: Deuterium and carbon-13 NMR of specifically labeled benzenehexoyl hexa-*n*-hexanoate in the various solid-state phases are reported. The spectra exhibit dynamic line shapes which change discontinuously at the phase transitions. The results are interpreted in terms of sequential "melting" of the side chains on going from the low-temperature solid phases IV, III, etc., toward the liquid. In phase IV the molecules are very nearly static, except for fast rotation of the methyl groups about their C_3 axes. The results in phase III were quantitatively interpreted in terms of a two-site isomerization process involving simultaneous rotation by 95° about C_1-C_2 and transition from *gtg* to *g'g't* (or equivalently *g'tg'* to *ggt*) for the rest of the chain. The specific rate of this reaction at 0 °C is $\sim 10^5$ s^{-1}. In phase II additional chain isomerization processes set-in which were, however, not analyzed quantitatively. Further motional modes, involving reorientation of whole chains about their C^{ar}-O bonds, appear on going to phase I. In all solid phases the benzene ring remains static.

I. Introduction

Discotic mesogens are liquid crystalline compounds whose molecules consist of a flat central core to which several (usually six) aliphatic side chains are bonded via ethers, esters, or other linkages.[1,2] The orientational order of the central core in the liquid-crystalline phase is generally quite high, but the side chains are highly disordered.[3] Several of these discotic compounds were shown to undergo a succession of solid-solid transitions, as a function of temperature below the mesophase or normal liquid regions.[4-8] An example of this behavior is exhibited by homologues of the benzenehexoyl hexa-*n*-alkanoate series (hereafter referred to as BHA*n*, where *n* designates the number of carbons in each of the side chains, see Figure 1). Detailed thermodynamic measurements on the homologues with $n = 6$, 7, and 8 were recently published[4-7] and interpreted in terms of step-wise "melting" of the side chains. However, these measurements do not provide direct information on the nature of the melting process. In favorable cases this type of information may be obtained from ^{13}C or ^{2}H NMR of specifically labeled species, and in the present paper we present such a study for the BHA6 homologue. Although, in pure form, this compound does not exhibit a mesophase[9,10] the general pattern of its solid-solid transitions is similar to that of the $n = 7$ and 8 homologues which are mesogenic.

The phase diagram of isotopically normal BHA6 is given in the upper row of Table I. There are four solid phases labeled IV, III, II, and I with increasing temperature. The transitions between them are all first order and accompanied by large transition entropies. On the basis of thermodynamic and IR measurements it was speculated[5] that the phase transitions reflect the following "melting" sequence of the side chains: Starting from a rigid all-trans structure in phase IV, the transition to phase III is accompanied by the onset of methyl group rotations, in phase II methylenes 5 and 4 attain full disorder, and in phase I methylene 3 starts to reorient. According to this model, only in the liquid state do the rest of the chain carbons undergo complete conformational disorder (in addition to overall rotational and translational disorder). We show below that although the phase transitions are indeed associated with chain melting the details are entirely different.

Table I. Phase Transition Temperatures (K) of the Various BHA6 Isotopomers

	IV	III	II	I	iso
BHA6[a]	251.58	291.46	348.27	368.74	
BHA6-*2-d*	254.60	291.00	352.00	366.80	
BHA6-*3-d*	250.40	289.80	350.70	367.00	
BHA6-*4-d*	247.90	289.00	348.80	368.20	
BHA6-*5-d*	248.50	291.30	349.20	368.00	
BHA6-*6-d*	249.50	287.50	347.20	366.20	

[a] Transition temperature of the isotopically normal compound.

[†] The Weizmann Institute of Science.
[‡] Max-Planck-Institut für Medizinische Forschung.

(1) Billard, J. In *Liquid Crystals of One and Two Dimensional Order*; Helfrich, W., Heppke, G., Eds.; Springer-Verlag: Berlin, 1980; p 383.
(2) Dubois, J. C.; Billard, J. In *Liquid Crystals and Ordered Fluids*; Griffin, A. C., Johnson, J. F., Eds.; Plenum: New York, 1984; Vol. 4, p 1043.
(3) Goldfarb, D.; Luz, Z.; Zimmermann, H. *Isr. J. Chem.* **1983**, *23*, 341. Luz, Z.; Goldfarb, D.; Zimmermann, H. In *Nuclear Magnetic Resonance of Liquid Crystals*; Emsley, J. W., Ed.; D. Reidel Publishing Co.: Dortrecht, Holland, 1985; p 343.
(4) Sorai, M.; Tsuji, K.; Suga, H.; Seki, S. *Mol. Cryst. Liq. Cryst.* **1980**, *59*, 33.
(5) Sorai, M.; Suga, H. *Mol. Cryst. Liq. Cryst.* **1981**, *73*, 47.
(6) Sorai, M.; Yoshioka, H.; Suga, H. *Mol. Cryst. Liq. Cryst.* **1982**, *84*, 39.
(7) Sorai, M. *Thermochim. Acta* **1985**, *88*, 1.
(8) Van Hecke, G. R.; Kaji, K.; Sorai, M. *Mol. Cryst. Liq. Cryst.* **1986**, *136*, 197.
(9) Chandrasekhar, S.; Sadashiva, B. K.; Suresh, K. A. *Praman* **1977**, *9*, 471.
(10) Chandrasekhar, S.; Sadashiva, B. K.; Suresh, K. A.; Madhusudana, N. V.; Kumar, S.; Shashidhar, R.; Venkatesh, G. *J. Phys. Colloque C3* **1979**, *40*, 3-20.

0002-7863/87/1509-7280$01.50/0

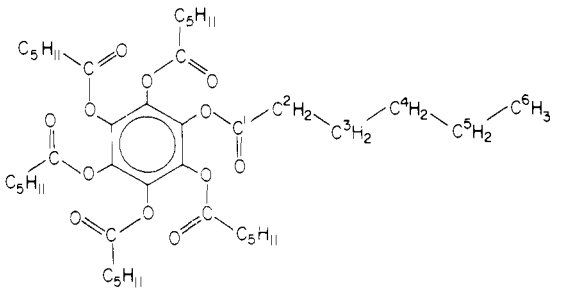

Figure 1. Molecular formula and numbering system of benzenehexoyl hexa-*n*-hexanoate (BHZ6) $C_6(OC(O)C_5H_{11})_6$.

Our conclusions are based on ^{13}C and ^2H NMR measurements of specifically labeled BHA6 species. Since no single crystals of this compound were available, the measurements were carried out on powder samples. The NMR line shapes of such samples are sensitive to the dynamical states of the molecules and on their structure. The basic principles for analyzing powder spectra have been reviewed[11-13] and a large number of worked-out examples have been published.[14-16] We therefore refer to the cited literature for the details of the analysis. The preparation of the compounds and other experimental details are described in section II, while the results are presented in section III. In section IV, we give a detailed analysis of the results of phase III, in terms of a specific isomerization process, and finally in section IV a general discussion is given.

II. Experimental Section

a. Material. Two types of isotopically labeled species of BHA6 were prepared: One type is labeled with ^{13}C and includes species specifically labeled at respectively the carboxyl carbon (BHA6-*1*-^{13}C) and the α-carbon (BHA6-*2*-^{13}C). The other type includes deuteriated species specifically labeled at the various carbons along the aliphatic chains.

The various BHA6 species were prepared by refluxing hexahydroxybenzene with the corresponding isotopically labeled hexanoyl chloride, followed by removing the excess acid chloride by vacuum distillation.[17]

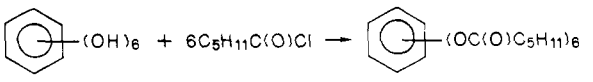

The residue was purified by column chromatography (silica gel, CH_2Cl_2/*n*-hexane 4:1) and recrystallized twice from ethanol (96%). Hexahydroxybenzene was prepared from tetrahydroxy-*p*-quinone (Aldrich) with $SnCl_2$ and HCl.[18] The hexanoyl chlorides were prepared from the corresponding acids by reaction with $SOCl_2$ in the usual manner.

[1-^{13}C]Hexanoyl chloride was prepared by carboxylation of *n*-pentyl-MgBr with $^{13}CO_2$ (obtained from $Ba^{13}CO_3$), while [2-^{13}C]hexanoyl chloride was prepared from *n*-butyl-MgBr with $^{13}CO_2$, followed by reduction, bromination, and carboxylation of the corresponding Grignard with $^{12}CO_2$.

Hexanoic-α-d_2 acid was prepared from *n*-hexanoic acid by exchange with D_2O containing an excess of NaOD at 200 °C.

Hexanoic-β-d_2 acid was prepared as follows: pentanoic-α-d_2 acid synthesized from the corresponding acid as above was reduced to pentanol-*2,2*-d_2 with $LiAlH_4$ followed by bromination to the corresponding bromide with red phosphorus and bromine. The Grignard compound of the latter was then carboxylated with CO_2 to give the hexanoic-β-d_2 acid.

For the preparation of hexanoic-γ-d_2 acid, propionic acid methyl ester (Aldrich) was first reduced with $LiAlD_4$ to propanol-*1,1*-d_2 and then converted to the corresponding Grignard compound as above. The latter was chain extended[19] with triethylene oxide to hexanol-*4,4*-d_2 followed by oxidation with $KMnO_4$/crown-6 in benzene to the desired product.

A similar procedure was used for hexanoic-δ-d_4 acid. Methylmalonic acid (Aldrich) was exchanged with D_2O and decarboxylated at 160 °C to propionic-α-d_2 acid. Reduction, bromination, and chain extension as above yielded the desired compound. The sequence of reactions was as follows:

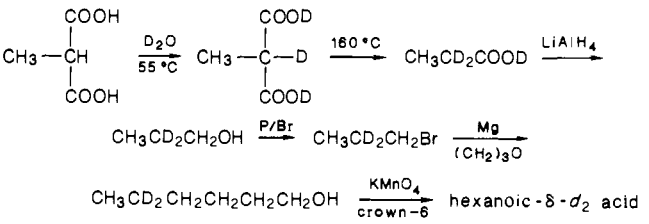

Hexanoic-ω-d_3 acid was obtained by starting with ethyl-*2,2,2*-d_3-malonic acid and chain extension with ethylene oxide instead of trimethylene oxide.

All the BHA6 isotopomers so obtained were checked by TLC and by ^1H NMR (at 360 MHz). From the latter the degree of the ^{13}C labeling was estimated to be 90 atom% and that of the deuterium ~98 atom%.

In Table I the transition temperatures of the various isotopomers are summarized and compared with those of the isotopically normal compound reported by Sorai et al.[4]

b. NMR Measurements. The ^2H and ^{13}C NMR spectra were recorded on a Bruker CXP300 spectrometer operating respectively at 46.07 and 75.46 MHz. High-power probes were used with a 10-mm horizontal solenoid coil for ^2H and a 5-mm coil for ^{13}C.

The deuterium spectra were obtained by the phase cycle quadrupole echo method[20] with intervals between the 90° pulses of 30 and 4–7 μs. The recycling time was 1 to 2 and usually 500–1500 scans were required for satisfactory signal to noise.

The ^{13}C spectra were obtained from single pulse experiments with proton decoupling. Recycle time was 9 s, and between 1000 and 5000 scans were required.

The temperature was controlled with a Bruker B-VT1000 variable-temperature unit and its absolute value calibrated with a Fluke 2190 digital thermometer (estimated accuracy ±1 °C).

Table II. Parameters Used in the Simulation of the ^2H Spectra in Phases IV and III of the Various Specifically Labeled BHA6-*n*-*d*

	2d	3d	$4d_{st}$[a]	$4d_{dy}$[b]	5d	6d
q_0 (kHz)	170	150–165	150	140	150	52
γ_n (deg)	88	113	0	125	113	90
$1/T_2$ (kHz)[c]	5.0	4.0	8.0		4.0	4.0

[a] Static component. [b] Dynamic component. [c] These line widths apply to the simulation of the static spectra of phase IV. For the dynamic spectra of phase III a common line width of 4 kHz was used throughout except for the end methyl deuterons for which a value of 2 kHz was employed.

III. Results and Discussion

As a general introduction to the experimental results we show in Figure 2 typical ^2H and ^{13}C spectra for each of the deuteriated species and for BHA6-*1*-^{13}C in the various solid phases. It may be seen that all the ^2H spectra in phase IV, except the end methyl deuterons, correspond very nearly to the rigid limit. This follows from the shape as well as from the overall width (~240 kHz) of the phase IV spectra. The distortion in these line shapes relative to an ideal powder spectrum is partly due to the finite width of the radio frequency pulses, but to a certain degree it is also due to the presence of slow motions. This is manifested in the relatively large and unequal $1/T_2$'s needed to simulate the spectra of the various methylenes in this phase (see Table II). The shape of the end-methyl spectrum is typical of a uniaxial quadrupole tensor, but its overall width is about $^1/_3$ of that of the methylenes, indicating that fast methyl group rotation about their C_3 axes already occurs in phase IV.

The ^{13}C spectrum of carbon-1 is characteristic of an axial chemical shift tensor and its overall width (135 ppm) corresponds

(11) Mehring, M. In *NMR-Basic Principles and Progress*, Diehl, P., Fluck, E., Kosfeld, R., Eds.; Springer-Verlag: Berlin, 1976.
(12) Griffin, R. G. *Methods Enzymol.* **1981**, *72*, 108.
(13) Spiess, H. W. *Colloid Polym. Sci.* **1983**, *261*, 193.
(14) Schwartz, L. J.; Meirovitch, E.; Ripmeester, J. A.; Freed, J. H. *Chem. Phys.* **19xX**, *87*, 4453. Rice, D. M.; Wittebort, R. J.; Griffin, R. G.; Meirovitch, E.; Stimson, E. R.; Meinwald, Y. C.; Freed, J. H.; Scheraga, H. A. *J. Am. Chem. Soc.* **1981**, *103*, 7707.
(15) Müller, K.; Meier, P.; Kothe, G. In *Progress in NMR Spectroscopy* **1985**, *17*, 211.
(16) Vega, A. J.; Luz, Z. *J. Chem. Phys.* **1987**, *86*, 1803.
(17) Nelfert, I. E.; Bartos, E. *J. Am. Chem. Soc.* **1943**, *65*, 177.
(18) Fatiadi, A. J.; Sager, W. F. *Organic Synthesis*; Wiley: New York, 1973; Collect. Vol. V., p 595.
(19) Searles, S. *J. Am. Chem. Soc.* **1951**, *73*, 124.
(20) Davis, J. H.; Jeffrey, K. R.; Bloom, M.; Valic, M. I.; Higgs, T. P. *Chem. Phys. Lett.* **1976**, *42*, 390.

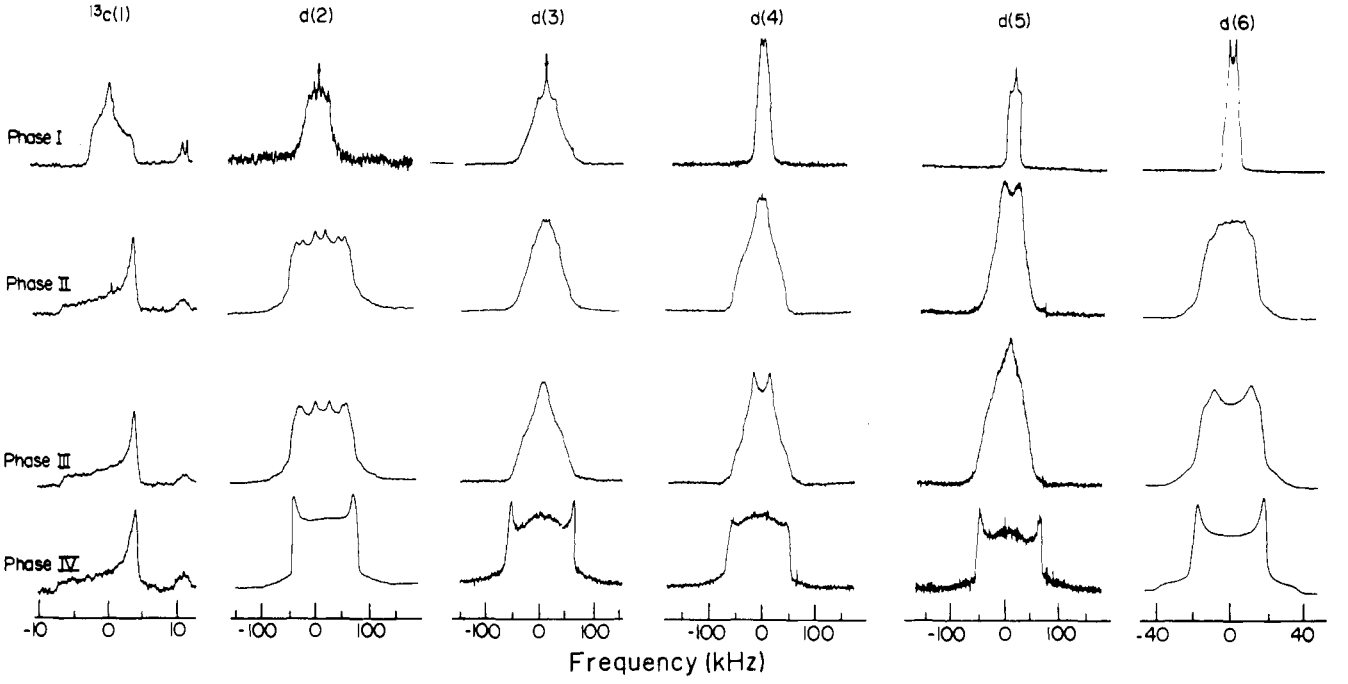

Figure 2. Representative ^{13}C and ^{2}H NMR spectra of specifically labeled BHA6 isotopomers in the various solid phases of BHA6.

to a rigid carboxyl carbon.[21-25] The shape of this spectrum remains unchanged throughout phases III and II but changes discontinuously on going to phase I. This indicates that the part of the chain involving the carboxyl carbon remains fixed with respect to the crystal frame in all solid phases except phase I. The situation is quite different for the rest of the chain as manifested by the pronounced line shape changes of the methylene (and methyl) deuteron spectra which take place already on going from phase IV to III and further changes when transition to higher phases takes place. We note, however, that the overall width of the spectra in phases IV, III, and II remains fairly constant and reduces drastically only on transition to phase I, which is also accompanied by changes in the ^{13}C spectra of carbon 1. This behavior suggests that in phases III and II the melting of the side chains involves highly restrictive jumps between a small number of well-defined conformations, while in phase I considerably more chain disorder sets in. We shall also see that in none of the solid phases does reorientation of the benzene ring occur (on the NMR time scale).

In the following we attempt to interpret the experimental results in terms of possible chain isomerization dynamics. In practice we were able to quantitatively analyze the spectra in phase III (in addition to those of phase IV), while for phases II and I only qualitative conclusions on the chain dynamics could be derived. We start with a discussion of the ^{13}C spectra, before turning to the deuterium results.

a. ^{13}C of BHA6-*1*-^{13}C. Two representative ^{13}C spectra of the carboxyl labeled BHA6 isotopomer, below and above the transition to phase I, are shown in Figure 3. As indicated above the low-temperature spectrum that remains unchanged in all phases below phase I is typical of a powder line shape due to a uniaxial, $\eta = 0$, chemical shift tensor. Its overall width of 135 ppm corresponds to that of a rigid carboxyl group, indicating that in all low-temperature phases no reorientation involving the carbonyl carbon, and for that matter of the whole benzene ring, takes place.

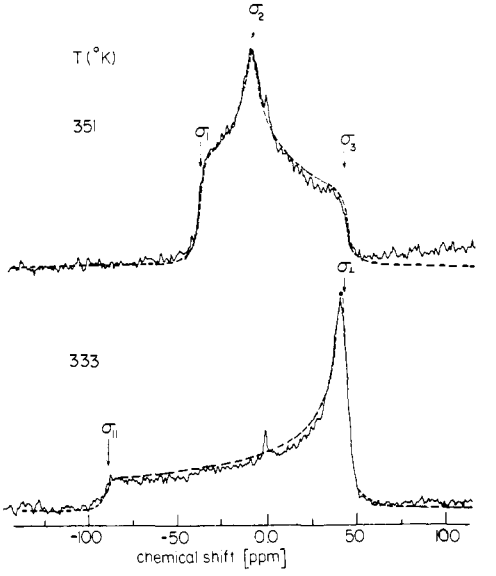

Figure 3. Proton-decoupled ^{13}C NMR spectra of BHA6-*1*-^{13}C at 60 and 78 °C corresponding respectively to phases II and I. The solid lines are experimental spectra while the dashed lines are calculated. These correspond to $\sigma_\parallel = -89.0$, $\sigma_\perp = 46.1$ ppm (relative to the center frequency) for the low-temperature phase and $\sigma_1 = -37.7$, $\sigma_2 = -8.4$ ppm, $\sigma_3 = 46.1$ ppm for the high-temperature phase ($1/T_2 = 2.5$ kHz).

On raising the temperature through the phase II to phase I transition, a discontinuous change in the line shape occurs, resulting in a biaxial spectrum with essentially the same average chemical shift and an asymmetry parameter $\eta = (\sigma_1 - \sigma_2)/(\sigma_3 - \sigma_{iso}) = 0.64$. This change in the line shape is due to the presence of a fast dynamic process in phase I which does not occur in the lower phases. To identify its nature we note that σ_3 of the high-temperature phase is essentially equal to $\sigma_\perp$ in the low-temperature spectrum, indicating that whatever the motion responsible for the partial averaging of the ^{13}C chemical shift it must be such that one direction in the $\sigma_\perp$ plane is unchanged by the dynamics. From previous studies on analogous compounds it is known that this plane very nearly coincides with the $OC_1(O)C_2$ plane. Assuming that the motion corresponds to conformational changes involving reorientation about single bonds, two possible mechanisms need be considered: (i) One possibility is reorientation

(21) Blume, A.; Rice, D. M.; Wittebort, R. J.; Griffen, R. G. *Biochemistry* **1982**, *21*, 6220.
(22) Witterbort, R. J.; Schmidt, C. F.; Griffin, R. G. *Biochemistry* **1981**, *20*, 4223.
(23) Witterbort, R. J.; Blume, A.; Huang, T. H.; Das Gupta, S. K.; Griffin, R. G. *Biochemistry* **1982**, *21*, 3487.
(24) Blume, A.; Griffin, R. G. *Biochemistry* **1982**, *21*, 6230.
(25) Blume, A.; Witterbort, R. J.; Das Gupta, S. K.; Griffin, R. G. *Biochemistry* **1982**, *21*, 6243.

of the whole chain about the O–C_1(O) bond. It is known, however,[26,27] that the four atoms of the ester group, $C^{ar}OC_1(O)$ prefer a coplanar configuration and that 180° flips about the O–C_1 bond are associated with a high-energy barrier. This renders this mechanism highly unlikely. (ii) The other, more probable possibility is reorientation about the C^{ar}–O bond. To conform with the experimental result that $\sigma_3 = \sigma_\perp$ requires that the C^{ar}–O bond remains in the $\sigma_\perp$ plane of the carboxy carbon tensor, i.e., the $C^{ar}OC_1(O)$ moiety remains coplanar before and after the jump. It should be noted that reorientation about C_1–C_2 and other bonds in the chain most likely occurs concomitantly with the carboxyl group rotation, but this does not affect the carboxyl ^{13}C spectrum. In principle changes in the ^{13}C spectrum could also result from jumps of the whole BHA6 molecule; however, this mechanism is ruled out by the low entropy change associated with the phase II to phase I transition.[4]

To be more specific we adopt a simplified model by assuming that the dynamic process involves discrete jumps between two distinct conformations that are equally populated. Under these conditions in the fast jump limit, taking γ as the jump angle of the principal component of the chemical shift tensor, the average chemical shift components in terms of the static ones are given by

$$\sigma_3 = \sigma_\perp = -(1/2)\sigma_\parallel$$

$$\sigma_2 = \tfrac{1}{2}[3\sin^2(\gamma/2) - 1]\sigma_\parallel$$

$$\sigma_1 = \tfrac{1}{2}[3\cos^2(\gamma/2) - 1]\sigma_\parallel$$

$$|\eta| = |(\sigma_1 - \sigma_2)/\sigma_3| = 3\cos\gamma$$

where the σ's are measured relative to the isotropic shift, and in the last equation we take absolute values since the sign of η cannot be determined from the spectrum. Substituting the experimental result for η in phase I gives a jump angle of 78° or 102°. Since no single-crystal results are available we cannot tell how these angles are related to the molecular structure. Recalling, however, the discussion in the previous section, the process could, e.g., correspond to switching of the $OC_1(O)C_2$ plane by approximately ±50° (above and below the benzene plane) or switching between 50° and 130° (on the same side of the benzene ring).

It is not possible to derive kinetic parameters for the flipping process since there is complete averaging of the chemical shift tensor already at the lowest temperatures of phase I. From the fact that the spectra could be well simulated (dashed lines in Figure 3) with a $1/T_2$ value of 2.5 kHz we may derive a lower limit of 10^6 s^{-1} for the flipping rate in this phase, but the actual value could be considerably higher. There is also no way to tell from the NMR whether the flipping of the chains is independent or cooperative. Space-filling consideration may favor at least a certain degree of cooperation.

This motion will of course also affect the orientation of the rest of the chain, and as indicated above, additional conformational changes may simultaneously take place at other methylene positions. All this is reflected in a very drastic narrowing of all the deuterium spectra on going from phase II to I (see Figure 2).

Carbon-13 measurements were also performed on BHA6-*2*-^{13}C; however, the overall width of the spectrum was considerably smaller and accordingly the changes in its line shape much less pronounced. More detailed information on this and the other aliphatic carbons in the low-temperature phases could be obtained by analyzing the deuterium spectra of the specifically deuteriated BHA6 isotopomers, and we now turn to these results.

b. ^2H NMR of Deuteriated BHA6. We have seen in Figure 2 that the transition from phase IV to phase III is accompanied by changes in the line shape of the deuterium signals from all sites along the aliphatic chain. Moreover the line shapes in phase III do not correspond to the fast motion limit but rather to the intermediate dynamic regime. We now attempt to interpret these spectra in terms of specific dynamic jump models. For simplicity we assume that for each deuteron they involve just two sites of equal populations. This yields for the various deuterons estimates for a corresponding jump angle and jump rate. The latter parameter turned out to be nearly equal for all deuterons (at least in phase III), suggesting that the observed dynamics correspond to a single well-defined isomerization process involving jumps between two distinct chain conformations. In section IV we analyze the results in terms of a possible pair of such exchanging conformations.

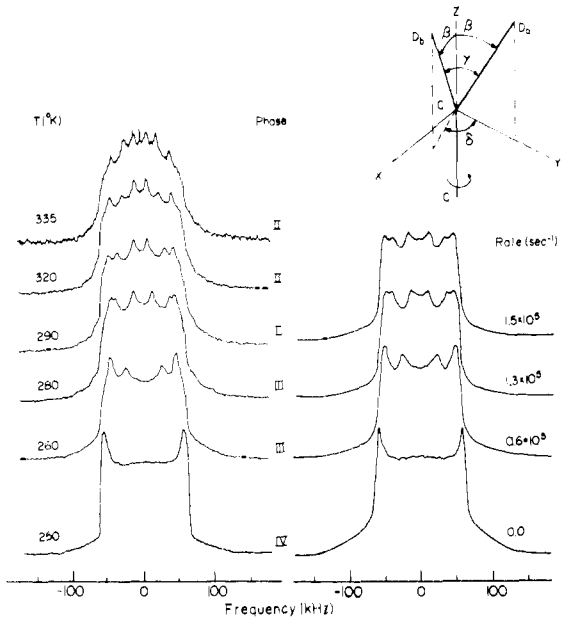

Figure 4. Left: ^2H NMR spectra of BHA6-*2*-*d* as a function of temperature in the solid phases IV, III, and II. Right: simulated spectra using the two site jump model with the parameters given in Table II and specific rates as indicated in the figure. Insert: schematic diagram of the geometrical relation between the ∠CCD (β), the C–D jump angle (γ), and the corresponding C–C dihedral bond rotation angle (δ).

BHA6-*2*-*d*. Deuterium NMR spectra of BHA6-*2*-*d*, i.e., of the α-deuteriated BHA6, as a function of temperature are reproduced on an expanded scale in the left column of Figure 4. The spectrum in phase IV (at 250 K) corresponds very nearly to the rigid limit of an axially symmetric quadrupole tensor with e^2qQ/h = 170 kHz. In simulating this spectrum it was however found necessary to assume a relatively large natural line width ($1/T_2$ = 5 kHz, see Table II) to best fit the experimental result (see bottom spectrum in the right column of Figure 4), suggesting that some slow motion does already occur in this phase. For the simulation of this and other spectra to be described below, the effect of the finite pulse width was incorporated in the calculation by convoluting the theoretical powder spectrum with an appropriate shape function.[28]

As the temperature is raised through the phase IV to phase III transition, a discontinuous change in the line shape takes place, resulting in more structured spectra whose shape varies with temperature. The line shape in this phase is reminiscent of dynamic spectra in which jumps between two sites occur. As for the ^{13}C case in the fast jump limit such samples exhibit powder spectra due to an asymmetric quadrupole tensor. Assuming that the static tensor is uniaxial with $q_0 = e^2qQ/h$, the principal components of the average tensor become

$$q_1 = (3/8)q_0[3\cos^2(\gamma/2) - 1]$$

$$q_2 = (3/8)q_0[3\sin^2(\gamma/2) - 1]$$

$$q_3 = -(3/8)q_0$$

$$|\eta| = 3\cos\gamma$$

(26) Pesquer, M.; Cotrait, M.; Marsau, P.; Volpilhac, V. *J. Phys.* **1980**, *41*, 1039.

(27) Cotrait, M.; Marsaum, P.; Pesquer, M.; Volpilhac, V. *J. Phys.* **1982**, *43*, 355.

(28) Bloom, M.; Davis, J. H.; Valic, M. I. *Can. J. Phys.* **1980**, *58*, 1510.

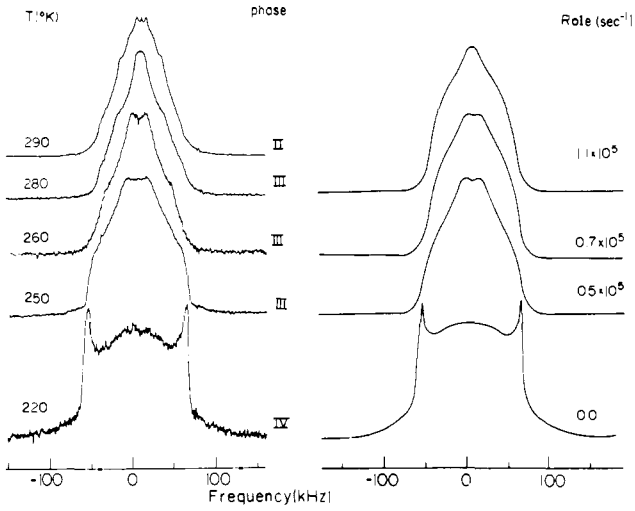

Figure 5. As in Figure 4 for BHA6-*3-d*.

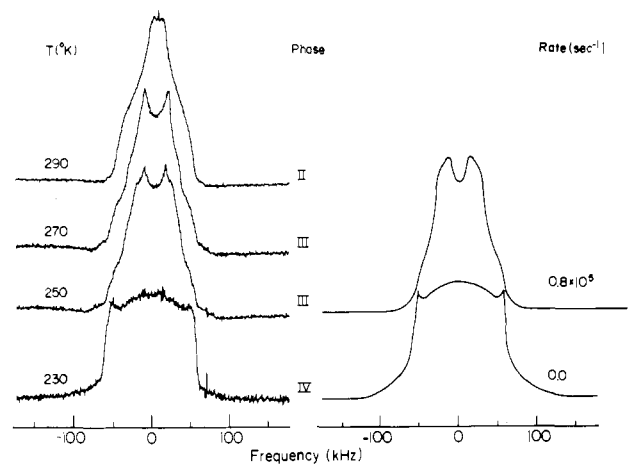

Figure 6. As in Figure 4 for BHA6-*4-d*.

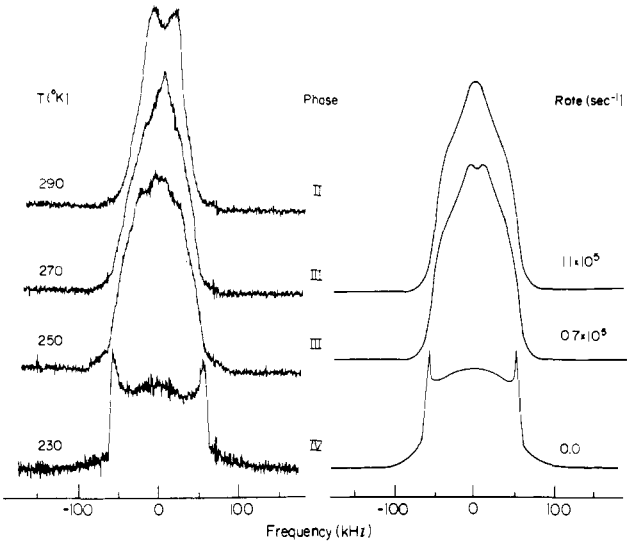

Figure 7. As in Figure 4 for BHA6-*5-d*.

where the principal axis 3 corresponds to the direction about which the jump takes place. Note that jumps over an angle γ and 180 − γ result in identical spectra, and likewise jumps of γ and 90 − γ, although in this case the assignment of axes 1 and 2 is reversed.

In the intermediate jump region the spectra are modified; however, the characteristic features of the average tensor appear already at relatively slow jump rates[29,30] allowing a preliminary estimate of the jump angle. The exact value of γ and the kinetic parameters were then determined by comparison of the experimental results with simulated dynamic spectra calculated according to the theory of Spiess and Sillescu.[31] Examples of such simulations which best fit the experimental spectra are shown in the right column of Figure 4. The parameters used in the simulation including the jump angle γ and the quadrupole interaction constant q_0 are given in Table II. The specific jump rates, k, used in the simulations are indicated in the figure.

In the discussion below we identify the jump angle γ with the switching in orientation of the C–D bonds, and we assume that this occurs as a result of conformational isomerization which involves reorientation about C–C bonds. Since we know from the carboxyl-^{13}C spectrum that in phase III the ester moiety is static, the switching of the α-deuterons can only be due to reorientation about the C_1–C_2 bond. The dihedral rotation angle of this bond, δ, is related to γ by (see insert in Figure 4)

$$\sin(\gamma/2) = \sin(\gamma/2)\sin\beta$$

where β is the ∠CCD that is taken as the complement of the tetrahedral angle, $\beta = 109.47°$. Taking $\gamma = 88°$ from Table II gives $\delta = 95°$.

Reasonably good fit between the experimental and simulated spectra could only be obtained for the experimental results in phase III. In the spectra of phase II new features appeared which could not be simulated by a simple two-site jump model. Apparently in this phase additional dynamic processes set in, but we were unable to come up with a model that would faithfully reproduce these results.

On further heating the sample to phase I another discontinuous change in the line shape occurs (see Figure 2) reflecting the onset of additional dynamical modes, in particular the one associated with the reorientation of the carboxyl group discussed above.

BHA-*3-d*. Deuterium NMR spectra of the BHA6-*3-d* species (β-deuteriated BHA6) in the various solid phases are shown in Figure 5. Their general appearance is similar to that of the α-deuteron, i.e., a nearly rigid spectrum in phase IV, and dynamically broadened spectra in the higher phases. The details are however quite different, in particular in phase III a dynamic spectrum with an average asymmetry parameter $\eta \sim 1$ is obtained which indicates a jump angle γ close to the tetrahedral value (or its 180° complement). Simulated spectra that fit the experimental results in this phase and the corresponding jump rates are shown in the right column of Figure 5. The other parameters used in the simulation are summarized in Table II. Note that essentially the same rates are derived as for the α-deuterons. We also emphasize that as for the α-deuterons a single spectrum is obtained for the two β deuterons, indicating that the dynamic process must involve identical jump angles for both hydrogens. This considerably restricts the possible isomerization mechanisms that need be considered for the interpretation of the results.

The spectra in phase II again exhibit new features that could not be reproduced by the simple jump model used for phase III. As for the α-deuterons the transition to phase I is accompanied by another discontinuous change in the line shape.

BHA-*4-d*. The spectra of γ-deuteriated BHA6 are shown in Figure 6. Although their general appearance is similar to that of the α and β deuterons they differ in several details. One point concerns the spectrum in phase IV whose simulation required a considerably larger $1/T_2$ value than for the α and β deuterons (see Table II). The second point concerns the spectra in phase III that appear as a superposition of two components, corresponding to a rigid and dynamic spectrum of about equal intensity. This indicates that whatever the dynamic process it must be such that would result in a net 0° (or 180°) reorientation of one of the γ deuterons. In fact satisfactory simulation of the spectra in phase III were only obtained by a superposition of a static spectrum and a dynamic one. The corresponding parameters are given in Table II.

(29) Alexander, S.; Baram, A.; Luz, Z. *Mol. Phys.* **1974**, *27*, 441.
(30) Baram, A.; Luz, Z.; Alexander, S. *J. Chem. Phys.* **1976**, *64*, 4321.
(31) Spiess, H. W.; Sillesau, H. *J. Mag. Reson.* **1981**, *42*, 381.

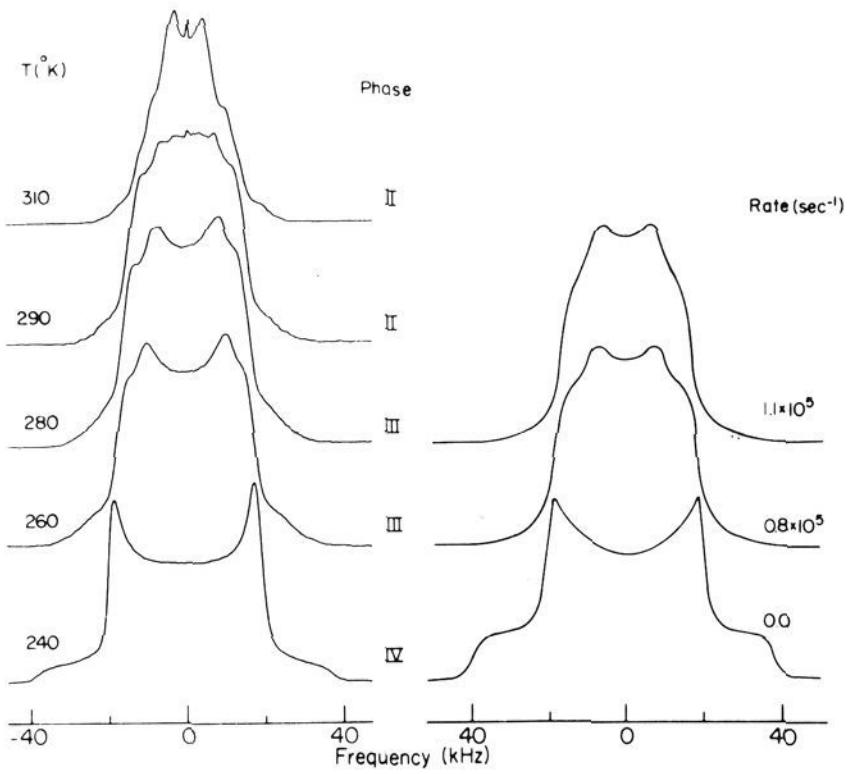

Figure 8. As in Figure 4 for BHA6-*6-d*.

BHA-*5-d* and BHZ6-*6-d*. The deuterium NMR spectra of the δ- and ω-deuteriated species and their best fit simulation are shown in Figures 7 and 8. In both cases the spectra in phase III correspond to a single dynamic line shape. The parameters used in simulating these spectra are summarized in Table II, and examples of calculated traces are shown in the right columns of Figures 7 and 8.

Note that the effective quadrupole interaction used for the end methyl (ω) deuterons is considerably smaller than that for the rest of the methylene deuterons. This is predominantly due to its fast rotation about the C_3 axis, but additional small-amplitude oscillations of the whole chain apparently also contribute. Such motions are probably also responsible for the drop of q_0 from 170 kHz for the α deuterons to 150 kHz for the δ ones (see Table II).

IV. Conformational Isomerization in Phase III

As indicated above, the fact that the deuterium line shapes of the various methylene (and methyl) groups (in phase III) could all be interpreted in terms of jumps between two equally populated sites with essentially the same jump rates suggests very strongly that the dynamic process involves isomerization between two distinct conformations of the side chains. In this section we attempt to identify conformations from the measured jump angles, γ, of the various deuterons. To do so we adopt the triisomeric model, i.e., we assume that the aliphatic chains consist of well-defined sequences of trans (t) and gauche (g,g') conformations. For simplicity we assume that all the aliphatic bond angles are tetrahedral so that only $\pm 120°$ dihedral rotations about the various C–C bonds are possible. The only exception is the C_1–C_2 bond which includes the nonaliphatic carboxyl carbon. We have already seen that this bond reorients by approximately 95° due to the isomerization process. The two interchanging isomers can thus be discussed in terms of two diamond lattices rotated relative to each other by 95° about the C_1–C_2 bond. With this model only five different γ values are allowed. They are the following: (i) $\gamma = 0$, when the C-D bond remains parallel to C_1–C_2 in both lattices. (ii) $\gamma = 88°$, when the CD bond is not parallel to C_1–C_2 but it retains its orientation within the corresponding diamond lattice. (iii) $\gamma = 109.47°$, when the isomerization corresponds to 120° rotation about a direction parallel to C_1–C_2, and either the original or the final orientation of the C–D bond is parallel to C_1–C_2. (iv and v) $\gamma = 128.1°$ or 23.5°, when the isomerization corresponds to rotation about a direction parallel to C_1–C_2 but neither the original nor the final orientations of C–D are parallel to C_1–C_2. The effective reorientation about C_1–C_2 is then either $(120 + 95)°$ or $(120 - 95)°$, corresponding to $\gamma = 128.1°$ (iv) or 23.5° (v), respectively. Referring to Table II we note that indeed only angles close to those listed above emerged from the analysis of the experimental data. Given these results we searched

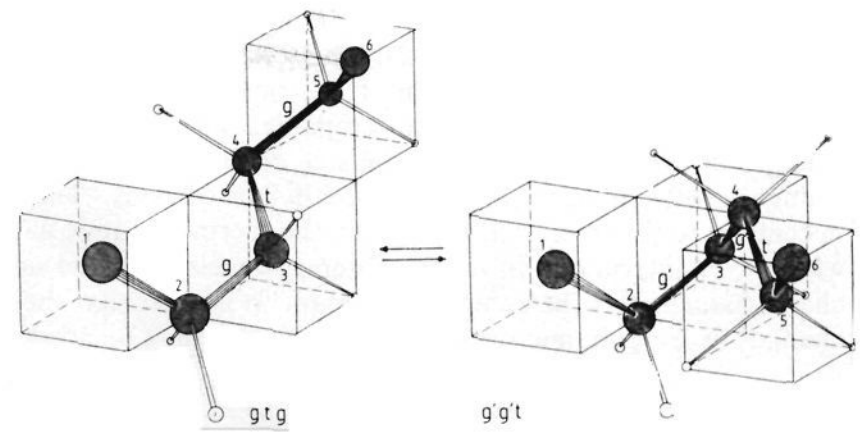

Figure 9. The two chain conformations within appropriate cubic lattices which are found to interconvert in phase III. The 95° rotation about C_1–C_2 is not included in the drawing.

for possible pairs of conformations that match the experimental observations. The scheme that best fit the experimental findings is shown in Figure 9. In the following we construct it in a stepwise manner using the rules summarized above.

For the β deuterons we find (Table II) $\gamma = 113°$ which within our experimental accuracy we identify with the tetrahedral angle. By checking various pairs of conformations for the C_2–C_3 bond it follows that only if one is g and the other g' will the isomerization result in a tetrahedral switch for both β C–D bonds. This situation corresponds to case iii, and it is independent of the dihedral rotation angle of the C_1–C_2 bond. In Figure 9 we identified the g and g' conformations with the pre- and post-jump states of the C_2–C_3 bond.

Proceeding to the γ-deuterons we recall that one of these deuterons remained invarient (case i above), while for the second deuteron $\gamma = 28.3°$ which is close to the 23.5° of case iv. There is one pair of configurations for the first three carbons which is consistent with this result, i.e., $gt \rightarrow g'g'$ (and of course equivalently $g't \rightarrow gg$). For the δ-deuterons we find again that γ equals approximately the tetrahedral angle. The only possible pair of conformations for the C_3–C_4 bond consistent with this result is $gtg \rightarrow g'g't$ as indicated in Figure 9 (or equivalently $g'tg' \rightarrow ggt$).

This scheme also fixes the orientation of the methyl groups. As may be seen the orientation of the methyl C_3 axis remains colinear with one of the α-deuterons before and after the jump. Consequently, the methyl deuterons must have the same γ values as the α deuterons, as is indeed found experimentally (see Table II).

V. Discussion

The deuterium NMR results presented above provided some detailed information on the dynamic states of the aliphatic side chains in the various solid-state phases of BHA6. They show that in the lowest temperature phase (IV), there is very little motion of the aliphatic segments on the NMR time scale, although they are certainly not completely rigid. This follows from the large $1/T_2$ values required to simulate the spectra in this phase (Table II). The exact mechanism of this relaxation is however not clear. Note that it results in unequal broadening of the various deuteron peaks.

The transition to phase III is accompanied by a discontinuous change in the dynamic state involving exchange between two well-defined conformations. Whether this exchange occurs between chains on the same molecule or involves two different molecules cannot be decided from the present results, although the former possibility appears more likely from spacial considerations. The rate of this process at 0 °C is approximately 10^5 s^{-1}; however, the accuracy of the results and the narrow temperature range over which phase III is stable made it impossible to determine accurately its activation energy. It is interesting to note in this connection that the two exchanging isomeric forms in phase III occupy very similar voids, making it very easy for the isomerization process to take place even in the solid state. This can be seen from the drawings in Figure 9, if the 95° rotation about C_1–C_2 is added. It thus appears that at least in the present case the triisomeric model, which is commonly used in fluids, also applies to crystalline phases.

Although we did not yet succeed in interpreting the details of the motions which take place in the other phases several general conclusions can already be drawn. In particular it appears that the solid-solid transitions are accompanied by discontinuous changes in the dynamic state of the side chains and that these changes involve in each case all the methylene carbons. This is in contrast to the interference based on the thermodynamic data which were interpreted in terms of stepwise melting of the side chains,[4] starting at the end methyl group. It is clear that these changes in the dynamic state of the side chain must be accompanied by changes in the molecular packing and of the crystal structure during the respective phase transitions. Such data are however not yet available for BHA6 in its various phases.

Acknowledgment. This research was supported by the United States-Israel Binational Science Foundation, Jerusalem. E.L. is a recipient of a Sir Charles Clore Post-Doctoral Fellowship.

Registry No. BHA6, 65201-69-6; BHA6-*2-d*, 110473-71-7; BHA6-*3-d*, 110473-72-8; BHA6-*4-d*, 110473-73-9; BHA6-*5-d*, 110473-74-0; BHA6-*6-d*, 110473-75-1.

Reduction of the Binuclear Iron Site in Octameric Methemerythrins. Characterizations of Intermediates and a Unifying Reaction Scheme

Linda L. Pearce,[†] Donald M. Kurtz, Jr.,*[†] Yao-Min Xia,[‡] and Peter G. Debrunner[‡]

Contribution from the Department of Chemistry, Iowa State University, Ames, Iowa 50011, and Department of Physics, University of Illinois, Urbana, Illinois 61801.
Received December 17, 1986

Abstract: Three oxidation levels are observed during reduction of the binuclear iron site in hemerythrin (Hr), namely, met [Fe(III),Fe(III)], semi-met [Fe(II),Fe(III)], and deoxy [Fe(II),Fe(II)]. Using absorption, EPR, and Mössbauer spectroscopies, we have characterized the two kinetically identifiable intermediates observed during the three stages of reduction of met- to deoxyHr. Our results establish for the first time the following characteristics about reduction of the iron sites in octameric metHr's by inorganic reducing agents between pH 6.3 and 8.2: (i) The latter two stages of reduction of *Phascolopsis gouldii* metHr have rate constants very similar to those previously published for *Themiste zostericola* Hr; these rate constants are independent of both concentration and nature of the reducing agent. (ii) The extent of antiferromagnetic coupling in the first-stage product, $(semi\text{-}met)_R$Hr, is ~5 times lower than that in metHr. (iii) The second-stage product consists of a mixture of deoxy and met oxidation levels; the latter we label met′ because of its inability to bind N_3^- and its unusual Mössbauer parameters. (iv) When an excess of reductant is used, ~70% of the iron sites in the second-stage product is at the deoxy level. (v) There are no detectable effects of D_2O on the rates of reduction. From these characterizations we propose a scheme for reduction of the iron site in Hr that unifies our results with those from several previous studies. A novel premise implied by our scheme is that only the iron atom closer to the outer surface of each subunit in the octamer is reduced by "outer-sphere" reagents. Thus, the product of the first stage of reduction, $(semi\text{-}met)_R$Hr, has this outer iron atom reduced. Reduction beyond the semi-met level requires electron exchange within the binuclear iron site such that the outer iron atom becomes reoxidized. A conformational change, during which this electron exchange occurs, is proposed to be the rate-determining step for the second stage. Relatively rapid reduction to deoxy can then occur directly either by the inorganic reagent or by disproportionation. Thus, these latter two processes are both conformationally controlled. According to our scheme, the proportions of met′ and deoxy in the second-stage product are determined by the relative rates of direct reduction vs disproportionation. The third stage we propose consists of rate-determining conversion of met′Hr back to metHr, after which normal reduction kinetics resume. The proposed scheme appears to be applicable to reduction of the iron site in monomeric metmyoHr as well. Our results provide a context for understanding reduction of the iron site in Hr by the apparent physiological reducing agent, cytochrome b_5.

Hemerythrin (Hr) is a respiratory protein found in several phyla of marine invertebrates. The protein from most species consists of an octamer of essentially identical subunits, each of which contains a binuclear non-heme iron oxygen-binding site.[1] A variety of physical studies, including X-ray crystallography,[2] and comparisons to synthetic complexes[3-5] have given a clear picture of the structural and electronic properties of this unique site. The structure of the iron site in [Fe(III),Fe(III)]metHr that has emerged from these studies has one six-coordinate iron atom, Fe1, and one five-coordinate iron atom, Fe2. The two iron atoms are linked to the protein by terminal imidazole and bridging carboxylate ligands. A third bridging ligand is provided by solvent in the form of an oxo ion. The presence of the μ-oxo bridge mediates a high degree of antiferromagnetic coupling between

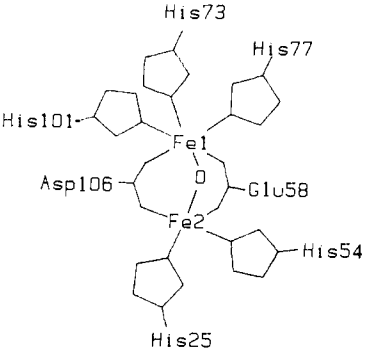

the high-spin ferric ions in metHr ($J = -134$ cm^{-1}), and this coupling is largely conserved in oxyHr.[6,7] The vacant site on Fe2

* Present address: Department of Chemistry, University of Georgia, Athens, GA 30602.
[†] Iowa State University.
[‡] University of Illinois.

(1) Klotz, I. M.; Kurtz, D. M., Jr. *Acc. Chem. Res.* **1984**, *17*, 17-22.

0002-7863/87/1509-7286$01.50/0